

# Lasing from fluorescent protein crystals

Heon Jeong Oh,<sup>1,2,5</sup> Malte C. Gather,<sup>1,3,5</sup> Ji-Joon Song,<sup>2,4,6</sup> and Seok Hyun Yun<sup>1,4,\*</sup>

<sup>1</sup>Wellman Center for Photomedicine and Harvard Medical School, Massachusetts General Hospital, 65 Landsdowne St., UP-5, Cambridge, MA 02139, USA

<sup>2</sup>Department of Biological Sciences, Korea Advanced Institute of Science and Technology, 291 Daehak-ro, Yuseong-gu, Daejeon 305-701, South Korea

<sup>3</sup>SUPA, School of Physics and Astronomy, University of St Andrews, St Andrews KY16 9SS, Fife, Scotland, UK

<sup>4</sup>Graduate School of Nanoscience and Technology (WCU), Korea Advanced Institute of Science and Technology, 291 Daehak-ro, Yuseong-gu, Daejeon 305-701, South Korea

<sup>5</sup>These authors contributed equally

<sup>6</sup>songj@kaist.ac.kr

\*syun@hms.harvard.edu

**Abstract:** We investigated fluorescent protein crystals for potential photonic applications, for the first time to our knowledge. Rod-shaped crystals of enhanced green fluorescent protein (EGFP) were synthesized, with diameters of 0.5–2  $\mu\text{m}$  and lengths of 100–200  $\mu\text{m}$ . The crystals exhibit minimal light scattering due to their ordered structure and generate substantially higher fluorescence intensity than EGFP or dye molecules in solutions. The magnitude of concentration quenching in EGFP crystals was measured to be about 7–10 dB. Upon optical pumping at 485 nm, individual EGFP crystals located between dichroic mirrors generated laser emission with a single-mode spectral line at 513 nm. Our results demonstrate the potential of protein crystals as novel optical elements for self-assembled, micro- or nano-lasers and amplifiers in aqueous environment.

©2014 Optical Society of America

**OCIS codes:** (140.0140) Lasers and laser optics; (160.0160) Materials.

---

## References and links

1. M. C. Gather and S. H. Yun, "Single-cell biological lasers," *Nat. Photonics* **5**(7), 406–410 (2011).
2. M. C. Gather and S. H. Yun, "Lasing from Escherichia coli bacteria genetically programmed to express green fluorescent protein," *Opt. Lett.* **36**(16), 3299–3301 (2011).
3. M. C. Gather and S. H. Yun, "Bio-optimized energy transfer in densely packed fluorescent protein enables near-maximal luminescence and solid-state lasers," *Nat. Commun* **5**, 5722 (2014).
4. F. Yang, L. G. Moss, and G. N. Phillips, Jr., "The molecular structure of green fluorescent protein," *Nat. Biotechnol.* **14**(10), 1246–1251 (1996).
5. R. Y. Tsien, "The green fluorescent protein," *Annu. Rev. Biochem.* **67**(1), 509–544 (1998).
6. J. R. Lakowicz, J. Malicka, S. D'Auria, and I. Gryczynski, "Release of the self-quenching of fluorescence near silver metallic surfaces," *Anal. Biochem.* **320**(1), 13–20 (2003).
7. D. L. Dexter and J. H. Schulman, "Theory of concentration quenching in organic phosphors," *J. Chem. Phys.* **22**(6), 1063–1070 (1954).
8. A. Royant, P. Carpentier, J. Ohana, J. McGeehan, B. Paetzold, M. Noirclerc-Savoye, X. Vernede, V. Adam, and D. Bourgeois, "Advances in spectroscopic methods for biological crystals. 1. Fluorescence lifetime measurements," *J. Appl. Cryst.* **40**(6), 1105–1112 (2007).
9. A. Royant and M. Noirclerc-Savoye, "Stabilizing role of glutamic acid 222 in the structure of enhanced green fluorescent protein," *J. Struct. Biol.* **174**(2), 385–390 (2011).
10. J. A. J. Arpino, P. J. Rizkallah, and D. D. Jones, "Crystal structure of enhanced green fluorescent protein to 1.35 Å resolution reveals alternative conformations for Glu222," *PLoS ONE* **7**(10), e47132 (2012).
11. T. Ansbacher, H. K. Srivastava, T. Stein, R. Baer, M. Merckx, and A. Shurki, "Calculation of transition dipole moment in fluorescent proteins—towards efficient energy transfer," *Phys. Chem. Chem. Phys.* **14**(12), 4109–4117 (2012).
12. M. Ormö, A. B. Cubitt, K. Kallio, L. A. Gross, R. Y. Tsien, and S. J. Remington, "Crystal structure of the *Aequorea victoria* green fluorescent protein," *Science* **273**(5280), 1392–1395 (1996).
13. A. Theisen, M. P. Deacon, C. Johann, and S. E. Harding, *Refractive Increment Data-Book for Polymer and Biomolecular Scientists* (Nottingham University Press, Nottingham, 2000).

---

Recent studies showed that the green fluorescent protein (GFP) in aqueous solution or in the cytoplasm of live cells constitutes an efficient optical gain medium [1, 2]. Lasing was observed by optically pumping GFP-expressing biological cells placed between a pair of

dielectric mirrors. More recently, it has been shown that dried GFP retains high quantum yield and forms solid-state films and rings of randomly packed GFP that support high gain and lasing [3]. Given the size of the GFP molecule (~2.4 nm along the short axis and ~4.2 nm along the long axis, 27-30 kDa in molecular weight) [4, 5], the concentration of GFP molecules in the solid state is approximately 15-45 mM. This concentration is several hundred to thousand times higher than the typical GFP concentration (1-100  $\mu$ M) in the cytoplasm of transfected cells. The particular molecular structure of GFP provides an optimal balance between high protein concentration and low concentration quenching, allowing near maximal brightness [3]. This is in stark contrast to typical low-molecular weight synthetic dyes that completely lose their ability to fluoresce when aggregated due to concentration quenching [6, 7].

When supersaturated under specific conditions, recombinant solutions of GFP can spontaneously form regular crystalline structures [4, 5]. Protein crystals are routinely used in x-ray crystallography to determine the molecular structure of the protein. The crystals consist of precisely ordered three-dimensional arrays of molecules with exactly defined composition and periodicity. Apart from their characteristic molecular absorption, they are optically transparent and do not scatter light. Therefore, GFP crystals are expected to generate significant optical gain. GFP crystals are known to be brightly fluorescent with emission spectra and excited state lifetimes similar to GFP solutions [8]. However, it is unknown how much concentration quenching takes place in GFP crystals. In this work, we synthesized crystals of enhanced GFP (EGFP) and investigated their properties as a fluorescent emitter and a laser gain medium.

EGFP is a variant of the wild type (wt) GFP with improved brightness and folding efficiency that are mainly due to mutations of two amino acids, namely S65T and F64L. Because EGFP differs from wt-GFP in several residues, our study started by determining suitable crystallization conditions for EGFP [9, 10]. EGFP was expressed from pET-28a-TEV-EGFP plasmid in *Escherichia coli* BL21 RILP in LB media. *E.coli* BL21 RILP was induced to express His-tagged recombinant protein at OD 0.631 with 1 mM isopropyl  $\beta$ -D-1-thiogalactopyranoside and cultured at 18 °C for 18 hours. The cells were sonicated in presence of Buffer A (50 mM Tris-HCl pH 8.0, 500 mM NaCl and 5% glycerol) containing phenylmethylsulfonyl fluoride. His-tagged protein was trapped and washed by Ni-bead in Buffer A containing 20 mM imidazole. It was further washed with Buffer B (50 mM Tris-HCl pH 8.0, 300 mM NaCl and 5% glycerol). Then two sets of elution were done with Buffer B containing 100 mM imidazole and 200 mM imidazole, respectively. After dialysis with a buffer containing 50 mM Tris-HCl pH 8.0, 100 mM NaCl, 1 mM DTT and 0.5 mM EDTA, the protein was further purified by ion exchange chromatography and gel filtration chromatography. The purified protein was concentrated to 17 mg/mL in a buffer containing 50 mM Tris pH 8.0 and 100 mM NaCl.

EGFP protein crystals were obtained by the hanging-drop vapor diffusion method. 1  $\mu$ L of the 17 mg/mL EGFP protein solution was mixed with 1  $\mu$ L of a buffer (mother liquor) containing 0.7 M ammonium sulfate, 0.1 M sodium citrate tribasic dihydrate pH 5.6, 0.8 M lithium sulfate monohydrate, and 10 mM phenol. Crystals were formed when either 10 mM manganese(II) chloride tetrahydrate or 10 mM sarcosine or 10 mM trimethylamine hydrochloride was added to the medium. The EGFP crystals had needle-like structures and accumulated in stellate clusters [Figs. 1(a)–1(c)]. Typical fully-grown crystals had lengths of 100-200  $\mu$ m and diameters of 0.5-2  $\mu$ m. After residual non-crystallized EGFP molecules in the medium were removed, the EGFP crystals were transferred to a clean buffer solution [Fig. 1(d)]. The crystals in the solution emitted bright green fluorescence when excited by laser light at 450-490 nm [Fig. 1(e)] or by femtosecond light at 800-1000 nm through two-photon absorption [Fig. 1(f)].

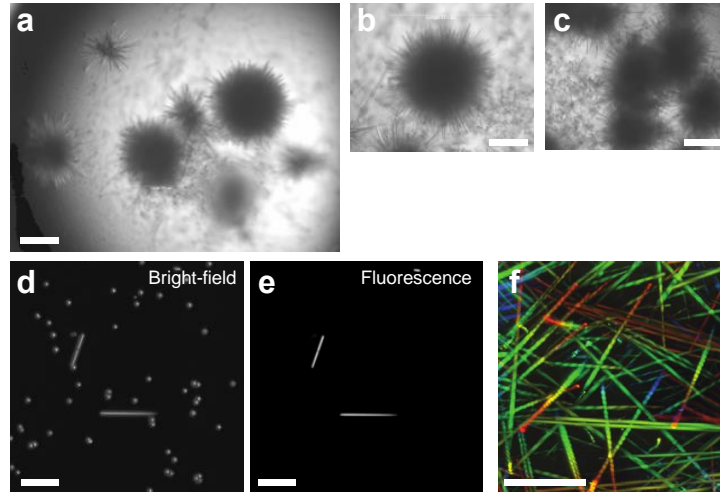


Fig. 1. EGFP crystals. (a-c) EGFP crystals formed by using trimethylamine hydrochloride (a), sarcosine (b), or manganese (II) chloride tetrahydrate (c). (d-e) EGFP crystals mixed with glass beads dispersed on a glass surface: (d) bright field micrograph; (e) fluorescence image. (f) Z-stack two-photon excited fluorescence image of EGFP crystals. Color represents depth (0-20  $\mu\text{m}$  from green to red). Scale bars, 100  $\mu\text{m}$ .

The emission intensity of the crystals was compared with aqueous solutions of EGFP at various concentrations [Fig. 2]. The fluorescence emission spectrum of the crystals was nearly identical to that from low-concentration EGFP solution. In terms of fluorescent emission per volume, the crystals were brighter than the EGFP solution samples at the highest concentration of 600  $\mu\text{M}$ , but the brightness was 7-10 dB lower than expected from the EGFP solution data when simply extrapolating low-concentration data.

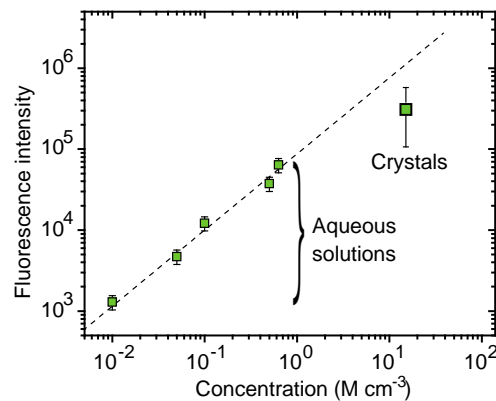


Fig. 2. Relative fluorescence intensity of EGFP crystals compared to EGFP solutions. The measurement was corrected for the thickness of each sample. Straight line is a linear extension of the data measured in EGFP solutions and may represent an ideal case without concentration quenching. The concentration in the crystal was assumed to be 15 mM based on the crystal structure. The measurement uncertainty (error bars) for the crystals was relatively large because of their small diameters.

This difference is primarily attributed to concentration quenching or the loss of absorbed photon energy to non-radiative quenchers. The 7-10 dB quenching in EGFP crystals is in fact much less than 20-30 dB quenching typically observed for small-sized synthetic dyes, such as rhodamine 6G (~480 Da) and pyromethene dyes (466 Da), which suffer from aggregation at high concentrations [3]. The relatively low quenching in EGFP crystals is attributed to the

molecular structure of fluorescent proteins, where the fluorophore is positioned in the center of a cylinder of beta-sheets [Fig. 3(a)]. Because of the protective shell, the fluorophore in a fluorescent protein is rigid and shielded from external influence. Small dyes can be quenched by the formation of non-fluorescent dimers or aggregates while the molecules are in the ground state (i.e. static quenching) or by short-range electron transfer from molecules in the excited state to specific quencher molecules. However, for fluorescent proteins both of these mechanisms contribute only minimally because the beta-barrel structure protects the fluorophores and separates fluorophores [3]. We expect that the dominant remaining quenching mechanism in EGFP crystals is a Förster resonant energy transfer (FRET) to non-fluorescent FP molecules that are denatured or misfolded.

Consider an EGFP molecule in the excited state (donor), which is surrounded by  $N$  nearest neighbor EGFP molecules at the ground state (acceptors) with a mean inter-fluorophore distance of  $R$  [Figs. 3(b) and 3(c)]. Although the precise quenching pathways are unknown, we may express the sum of the rates of all possible quenching processes as:

$$\sum k_i \equiv \chi \cdot (k_R + k_{NR}), \quad (1)$$

where  $k_R$  and  $k_{NR}$  denote the rates of radiative and non-radiative decay within the donor molecule, and  $\chi$  greater than 1 is a quenching factor. Let the rate of FRET from the donor to the acceptor fluorophore be  $k_{R,FRET}$ . Using the definition of the Förster radius  $R_F$  of a EGFP-EGFP pair,  $k_{R,FRET}$  can be expressed as:  $k_{R,FRET} = (k_R + k_{NR}) \cdot R_F^6 / R^6$ .

The total fluorescence intensity is given by summing the probabilities of having fluorescence emission from the  $n$ -th acceptor molecule after  $n$ -fold resonant energy transfer ( $n = 0 \dots \infty$ ):

$$I = C \cdot \frac{k_R}{k_{tot}} \sum_{n=0}^{\infty} \left( \frac{k_{R,FRET}}{k_{tot}} \right)^n = C \cdot QY \frac{1}{1 + \chi} \quad (2)$$

where  $C$  is a proportionality constant that is proportional to the EGFP concentration,  $k_{tot} = k_R + k_{NR} + \sum k_i + k_{R,FRET}$  is the total transition rate, and  $QY = k_R / (k_R + k_{NR})$  is the quantum yield of EGFP at low concentration. From the measurement shown in Fig. 2, we estimate  $\chi \approx 5$ -10.

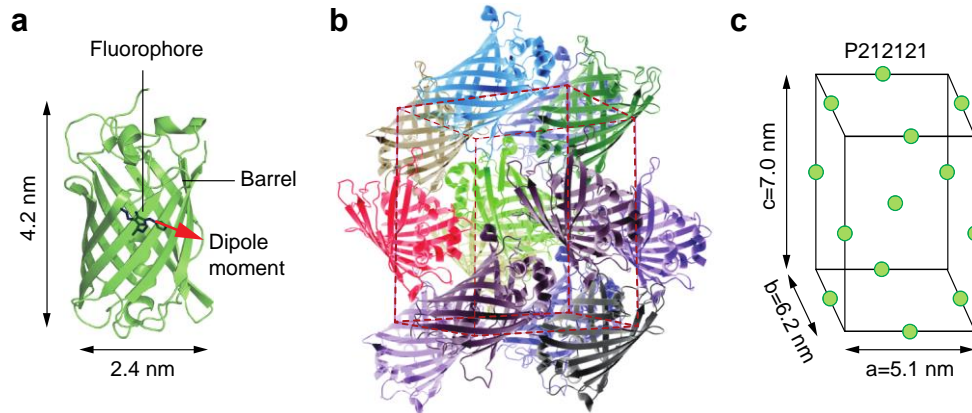


Fig. 3. Crystal structure. (a) GFP molecule drawn in a cartoon style. The permanent dipole moment (red arrow) is nearly parallel to the short axis of the  $\beta$ -barrel. The transition dipole moment of the fluorophore is at a small angle ( $\sim 13^\circ$ ) with respect to the long axis of the fluorophore [11]. (b) Illustration of an EGFP crystal in the most probable space group P212121 [12]. (c) Schematic of the EGFP crystal. Green spheres represent individual GFP molecules in the unit cell. For an excited molecule (donor), there are 12 nearest neighbors at similar, although not identical, distances, which can accept the excited state energy via FRET.

The high brightness of the EGFP crystals indicates their potential as novel gain medium. To demonstrate this, we used two dichroic mirrors with >99.5% reflectivity in the spectral range of 500 to 580 nm to form a Fabry-Perot-type laser cavity. To transfer a protein crystal from the original hanging droplet, 6  $\mu\text{L}$  of fresh mother liquor was added to the droplet to prevent NaCl from forming a salt crystal. The protein crystal was transferred to another 6  $\mu\text{L}$  of fresh mother liquor on a glass slide using a cryoloop (Hampton Research). The mother liquor was soaked up almost completely with a strip of paper (KimWipes, KimBerly-Clark) to remove any remaining protein solution and another 6  $\mu\text{L}$  of fresh mother liquor was added to the cluster of protein crystals. A small amount of glass beads with nominal diameter of 10 or 20  $\mu\text{m}$  was added to the liquor as spacer for the laser experiment. A droplet of the mixture of crystals and beads in clean buffer was applied to the surface of a dichroic laser mirror. Then, the other dichroic mirror was placed on top, forming a laser cavity [Fig. 4].

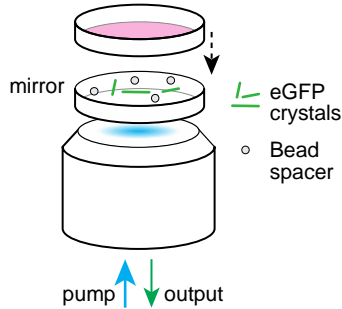


Fig. 4. Schematic of the experimental setup.

The crystal-containing resonator was placed on a 3-axis micro-stage to position a single selected protein crystal into the excitation spot of the pump laser. The pump light was provided from an optical parametric oscillator (Quanta Ray MOPO-700, Spectra Physics; pulse duration  $\sim 5$  ns, tuned to 485 nm) and delivered to the sample through a 40x objective. The pump light was focused to near the back focal plane of the objective to illuminate the entire crystal up to 200  $\mu\text{m}$  in length without having excessive unproductive excitation away from the crystal. The emission from the protein crystal was directed to both a CCD camera and a spectrometer (Andor, 0.1 nm resolution) to monitor the sample, the pump light, the output emission pattern and the spectral composition of the output.

Figure 5 shows the output characteristics of the protein crystal laser. The output energy in the 500-600 nm range increased sharply with increasing pump energy above the lasing threshold (66 nJ) [Fig. 5(a)]. Below threshold, the output spectrum was broad and modulated by the periodic spectral characteristic of the mirror resonator [Fig. 5(b)]. Above threshold, a single laser line appeared at 513 nm. These results provide evidence for the generation of laser light by the EGFP crystal. The quenching factor,  $\chi$ , in Eq. (3) depends on the radiative transition rate,  $k_R$ , which is enhanced by stimulated emission. Therefore, during laser oscillation the effect of concentration quenching on the laser output intensity might actually be less pronounced than for spontaneous fluorescence emission at low population inversion levels.

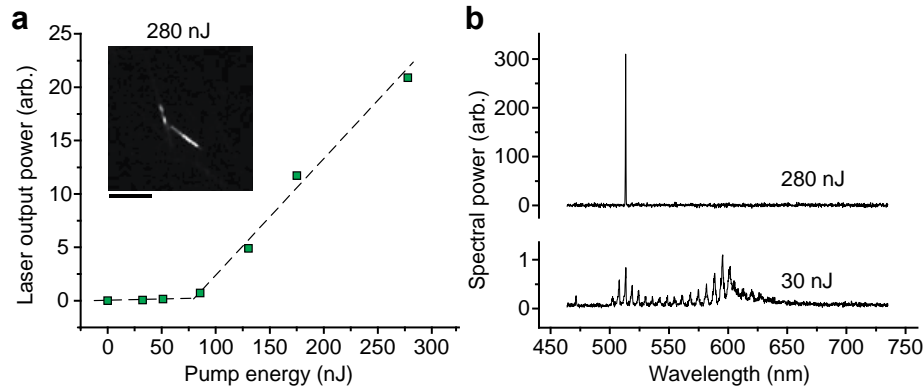


Fig. 5. Laser based on a protein crystal. (a) Laser output energy of a protein-crystal laser as a function of the pump energy; line, linear fit. Inset shows an image of the output emission at pump energy of 280 nJ. Scale bar, 50  $\mu\text{m}$ . (b) Output spectra at two different pump levels of 30 nJ and 280 nJ. The spectral power at 30 nJ is displayed with 100x magnification for easier comparison.

In conclusion, we have shown that fluorescent protein crystals can amplify light and serve as active medium for stimulated laser emission. We expect to achieve lasing from other types of fluorescent proteins, such as red fluorescent proteins like turboRFP. As an optical material, a fluorescent-protein crystal offers several advantageous properties, such as minimal light scattering and maximal concentration with an acceptable magnitude of self-quenching as well as its small sizes and self-assembling nature. Protein crystals bear potential for use as miniature laser sources in micro-phonic devices. The refractive index of a protein crystal ( $n = \sim 1.52$  [13]) is considerably higher than the surrounding medium. Therefore, a long rod-shaped protein crystal can be able to guide light and may serve as an amplified spontaneous emission source, a light-guiding amplifier or potentially even as a micro-rod laser cavity.

#### Acknowledgments

We thank Uhn-Soo Cho for discussion about crystal handling and Myunghwan Choi for taking two-photon fluorescence images of the crystals. This work was funded by the National Science Foundation (ECCS-1101947, EEC-1358296), the Korea National Research Foundation (R31-2008-000-10071-0), the KAIST-MGH Summer Internship Program, and the European Union Marie Curie Career Integration Grant (PCIG12-GA-2012-334407).